European Journal of Control (2008)4:308–320

DOI:10.3166/EJC.14.308–320

European Journal of Control

Optimality Properties and Driver Input Parameterization for Trail-braking Cornering

Efstathios Velenis[1,*], Panagiotis Tsiotras[2,**] and Jianbo Lu[3,***]

[1]School of Engineering and Design, Brunel University, Uxbridge, Middlesex, UB8-3PH, UK;
[2]D. Guggenhein School of Aerospace Engineering, Georgia Institute of Technology, Atlanta, GA 30332–0150, USA;
[3]Research and Advanced Engineering, Ford Motor Company, 20300 Rotunda Dr. Dearborn, MI 48124, USA

In this work we present an analysis of rally-racing driving techniques using numerical optimization. We provide empirical guidelines for executing a Trail-Braking (TB) maneuver, one of the common cornering techniques used in rally-racing. These guidelines are verified via experimental data collected from TB maneuvers performed by an expert rally driver. We show that a TB maneuver can be generated as a special case of the minimum-time cornering problem subject to specific boundary conditions. We propose simple parameterizations of the driver's steering, throttle and braking commands that lead to an alternative formulation of the optimization problem with a reduced search space. We show that the proposed parametrization of the driver's commands can reproduce TB maneuvers along a variety of corner geometries, requiring only a small number of parameters.

Keywords: Trajectory optimization, vehicle dynamics, technical driving, autonomous vehicles.

1. Introduction

The state of the art in autonomous ground vehicles was demonstrated during the 2005 DARPA Grand Challenge, where several teams raced their vehicles autonomously over 131.2 miles of unpaved road in the Mojave desert within 10 hours [1]. The winning team, from Stanford University, completed the course at an average speed of approximately 19 mph. It is envisioned that the next generation of autonomous ground vehicles will be able to travel autonomously faster than these moderate speeds, and perhaps as fast as human (expert) car drivers. It is therefore of interest to develop mathematical models and control algorithms that will be able to deal with the trajectory generation and tracking problem under high-speed and/or other abnormal (e.g., off-road, rough surface) driving conditions. In this paper we initiate such a program, starting with the investigation of the optimality properties of these expert driver techniques. Our ultimate objective is to use these highly specialized maneuvers in the overall control architecture.

The problem of trajectory planning for high-speed ground vehicles over rough terrain presents an enormous technical challenge. For paved roads some results do exist, obtained using numerical optimization [6, 7, 12, 18]. These results demonstrate that numerical techniques allow one to incorporate accurate, high order dynamical models, thus producing realistic results. On the other hand, these numerical optimization approaches are computationally intensive, and they cannot be readily implemented on-board the vehicle in real-time. Analytical approaches have also been proposed in the literature for minimum-time

*Correspondence to: E. Velenis, E-mail: efstathios.velenis@brunel.ac.uk
**E-mail: tsiotras@gatech.edu
***E-mail: jlu10@ford.com

Received 19 October 2007; Accepted 10 April 2008
Recommended by S.M. Savaresi, E.F. Camacho

control strategies for land vehicles along paths of fixed geometry [10, 13, 17, 19]. These analytical methodologies are computationally less intensive than numerical approaches. However, the assumptions used in these works tend to oversimplify the problem.

A new approach to real-time path planning of autonomous vehicles, which can be used to overcome the limitations of both numerical and analytical optimization techniques, has been developed in [8, 9] for aggressive autonomous operation of robotic helicopters. In these references the optimal trajectory is computed by scheduling on-the-fly a series of precomputed maneuvers from a maneuver library using a finite state machine (maneuver automaton). One is then able to perform real-time path planning by pasting together these maneuvers from the maneuver library. The scheme of [8, 9] is particularly appealing to the problem of path planning of high-speed off-road ground vehicles that mimic the aggressive driving techniques used by expert human drivers. Indeed, it has long been known that expert drivers competing in off-road racing (rally-racing) utilize a series of specialized aggressive maneuvers (Trail-Braking (TB), Pendulum turn, power oversteer, etc.) to control the vehicle at high speed during cornering. It is therefore natural to consider an approach similar to the one in [8, 9], whereby one computes off-line a collection of aggressive maneuvers and subsequently use them on-line for vehicle control in high-speed regimes. In this paper we present the details of one of the maneuvers in the maneuver library for high-speed control of wheeled vehicles. Note that unlike paved road racing or closed-circuit racing of high-performance vehicles (e.g., F1), to date there has been no concrete amount of work correlating driving techniques used by expert rally drivers with mathematical models. In order to achieve the previous task we therefore start with the use of empirical information collected from our interactions with expert rally race drivers, along with experimental results. We then develop a mathematical and computationally tractable framework that succinctly formalizes this empirical information and encapsulates the essential optimality features of these maneuvers.

In the following, we first present (Section 2) empirical guidelines for TB, one of the common cornering techniques used in rally racing. These guidelines are verified using data collected from tests performed by an expert rally driver. In Section 3 we introduce a low-order vehicle model that incorporates a sufficient level of fidelity to reproduce modes of operation in accordance to the empirical descriptions of rally maneuvers. Because of its low complexity, the model can be used efficiently within an optimization scheme. We use a nonlinear programming algorithm, in conjunction with the above vehicle model, to solve several cases of the minimum-time cornering problem. TB appears as the solution to the minimum-time problem subject to appropriate boundary conditions at the exit of the corner. Subsequently, in Section 4 we propose a simple parameterization of the driver's steering, braking and throttle control inputs for a TB maneuver, in accordance to the empirical guidelines and experimental data. We use the simplified description of the input signals in an alternative optimization scheme with a greatly reduced search space. This new optimization scheme allows us to reproduce TB maneuvers efficiently along a variety of corner geometries using a high fidelity vehicle model. Finally, the last section summarizes our conclusions.

2. Empirical Description of the TB Maneuver

Rally-racing has traditionally provided a research and development platform for improving the safety and performance of passenger vehicles. As an example, the development of All-Wheel-Drive road vehicles entered commercial production after the successful introduction of the Audi Quattro in rally racing in the 1980s. Despite these technological successes, the techniques and driving style of expert rally race drivers have not yet been fully analyzed via a rigorous mathematical framework, at least not in a way that it could help researchers to develop control systems that are able to operate a vehicle during extreme or abnormal driving conditions. This knowledge remains empirical and exclusive to a select few expert rally race drivers. In this article we initiate a study of expert rally driving techniques. We start by presenting empirical information on TB, one of the commonly used rally racing maneuvers.

2.1. Empirical Guidelines for TB

TB is a technique used by rally drivers to negotiate single corners at high speeds [14]. Typically, an average/novice driver negotiates a corner by first braking to regulate the speed, then by releasing the brakes and steering the vehicle along the corner, and finally by accelerating after the exit of the corner. In TB deceleration of the vehicle by braking continues even after steering has commenced. It is used when the approach speed to the corner is high.

Consider, for example, a 90 deg left corner as shown in Fig. 1. Approaching the corner at high speed from the outer edge of the road, TB begins by braking the

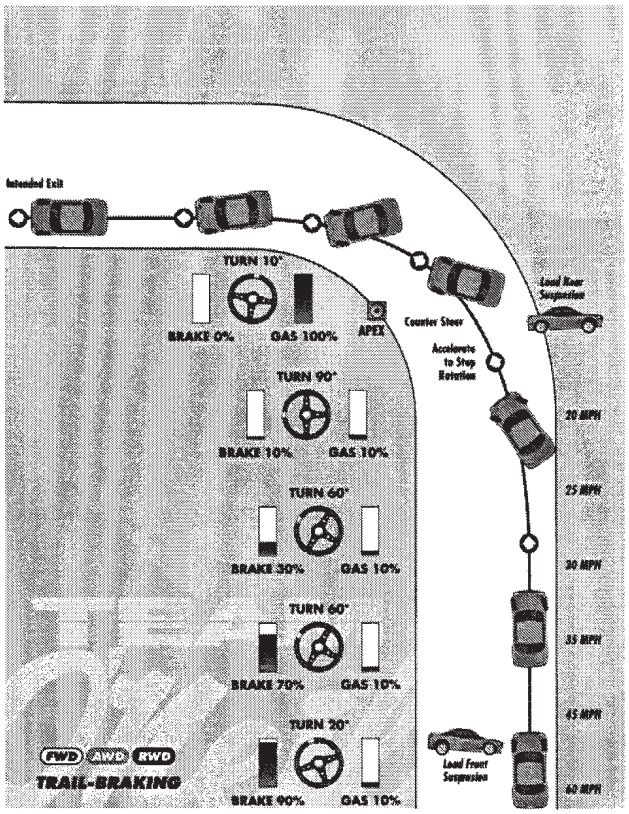

Fig. 1. Empirical description of the Trail-Braking maneuver; from [15].

vehicle without steering. The driver adjusts the brake pressure such that the maximum available friction is generated by the tires. This means that the maximum available deceleration is generated; subsequently, no friction for steering is available. As the vehicle approaches the corner, the driver starts steering the vehicle. In TB this is done by progressively releasing the brake (in order to allow cornering forces at the tires) and simultaneously–and progressively–increasing the steering angle. As the vehicle decelerates, the weight of the vehicle transfers from the rear axle to the front axle and thus, the front tires generate higher friction (cornering force) than the rear ones. Due to the increased cornering force at the front axle and decreased cornering force at the rear axle, the vehicle tends to oversteer and it rotates about the vertical axis counterclockwise, at a high rate. As the vehicle reaches the apex and its attitude is aligned with the exit of the corner, the driver accelerates and counter-steers (steers toward the opposite side of the corner) to stop the rotation of the vehicle and start the acceleration toward the exit of the corner. The acceleration causes the weight of the vehicle to transfer from the front axle to the rear axle. As a result, the rear tires generate more friction, resisting the counterclockwise rotation of the vehicle.

Fig. 2. The 340 BHP, 510 Nm, All-Wheel-Drive CPD Racing Subaru Impreza used during the tests.

Overall, TB involves high vehicle slip angles and yaw rates. This aggressive rotation brings the vehicle to a controllable, straight line driving state in a short distance after the corner, and allows the driver to react to unexpected changes in road conditions ahead of the corner, which are typical during off-road rally racing. The resulting trajectory ends up close to the inner limit of the road and is known as the late apex line [14].

2.2. Data Collection and Analysis

The above guidelines for a TB maneuver were verified using data collected during the execution of several TB maneuvers by Mr. Tim O'Neil, a five times US and North American Rally Champion and rally driving instructor. The test took place at the facilities of Team O'Neil Rally School and Car Control Center in Dalton, New Hampshire. The vehicle used was a Group A 2004 Subaru Impreza WRX STI (Fig. 2) owned by CPD Racing and prepared by ProDrive. The maneuvers were executed on gravel surface (typical friction coefficient $\mu = 0.5–0.6$).

The vehicle was instrumented with the following sensors (Fig. 3): An Oxford Technical Solutions RT3000 inertial measurement and GPS unit [2] to measure three-axes accelerations, three-axes rotational rates, and absolute vehicle position and heading. The RT3000 was provided by the Research and Advanced Engineering department of Ford Motor Company. Two string extension potentiometers were fitted on the steering column and the throttle cable to measure the steering wheel angle and throttle position respectively. In addition, a pressure transducer was placed at the brake line using a T-fitting to measure the brake pressure. More information on these sensors can be found in [3]. A DL2 data logger and GPS system [3] was used to collect the data from

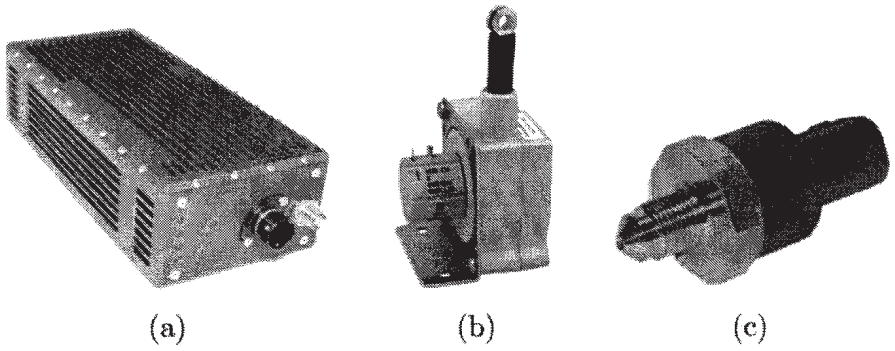

Fig. 3. (a) The RT3000 inertial measurement and GPS unit; (b) String extension potentiometer for steering wheel angle measurement; (c) Pressure transducer for brake pressure measurement.

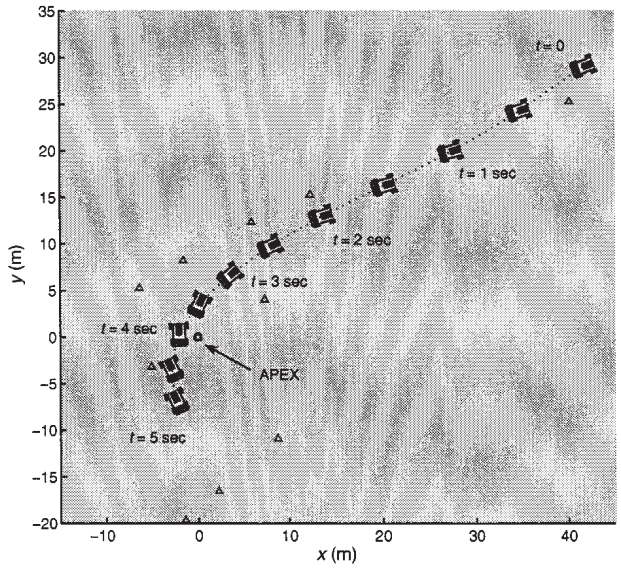

Fig. 4. A Trail-Braking trajectory reproduced from experimental data.

the potentiometers and the pressure transducer. The data from the RT3000 was directly logged to a portable PC.

The goal of the test was to capture the actions of the driver (steering, braking and throttle commands) and the resulting vehicle response as a rigid body, rather than internal dynamics dealing with the engine, transmission, brake, suspension and steering subsystems.

The test driver executed a TB maneuver around a tight corner, approximately 80–90 deg. Fig. 4 shows the trajectory of the vehicle using the absolute position and heading measurements. Cones were used to mark the limits of the road and the apex of the corner. These are denoted by triangles in Fig. 4. In this figure the origin has been moved to the apex of the corner. Fig. 5 shows the driver's steering, brake and throttle commands, normalized by the maximum steering position, brake pressure and throttle position measurements as

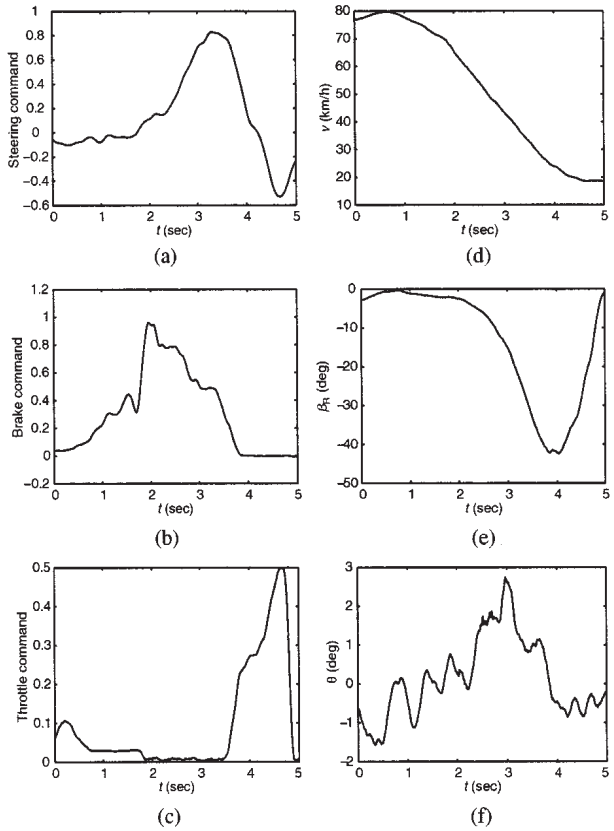

Fig. 5. Experimental data from Trail-Braking maneuver. (a) normalized steering command; (b) normalized braking command; (c) normalized throttle command; (d) vehicle speed; (e) vehicle slip angle at the rear axle; (f) vehicle pitch angle.

a function of time, as well as the vehicle speed v, the vehicle slip angle β_R at the rear axle and the vehicle pitch angle θ, in accordance to the ISO 8855 coordinate system.

The sequence of the driver's actions and the resulting vehicle response are summarized below:

During $0 \leq t < 2$ sec the driver regulated the speed to approximately 75–80, km/h, traveling in a straight line.

At $t = 2$ sec the car reached the 25 m mark (distance from the apex–Fig. 4) and the driver braked hard.
During $2 < t < 3.5$ sec the driver progressively released the brakes and increased the steering angle towards the direction of the corner. Deceleration of the vehicle resulted in normal load transfer from the rear to the front wheels, which can be seen from the increase of the pitch angle (Fig. 5(f)). As the rear axle load was reduced, the friction of the rear tires was also reduced and the vehicle started rotating counterclockwise, oversteering with increasing slip angle (Fig. 5(e)).
During $3.5 \leq t \leq 4$ sec the vehicle approached the apex of the corner at a high slip angle and the driver took action to stabilize the vehicle and exit the corner. The driver subsequently reduced the steering angle, progressively released the brakes and applied throttle.
During $4 < t \leq 5$ sec the driver counter-steered and progressively increased the throttle command. As the vehicle accelerated, the rear axle normal load increased, and hence so did the friction of the rear tires. The counterclockwise rotation was damped, the slip angle was reduced to zero and the vehicle accelerated straight while exiting the corner. For safety, and due to the limited space, the driver chose to accelerate only until the vehicle exited the corner, cutting-off the throttle just before the $t = 5$ sec mark.

The experimental data collected during the execution of the previous TB maneuver are in accordance to the empirical guidelines discussed in Section 1. That is, the driver applied progressively decreasing braking with increasing steering command, followed by counter-steering and progressive acceleration. The result was an aggressive cornering maneuver utilizing high vehicle slip angles.

3. Minimum-Time Cornering

In this section we reproduce the TB maneuver using numerical optimization. A low order vehicle model is introduced and the minimum-time problem for a 90 deg corner is formulated. The TB maneuver is reproduced as a special case of the optimal solution subject to certain endpoint boundary conditions.

3.1. Vehicle Model

In this section we introduce a vehicle model suitable for studying aggressive driving maneuvers such as TB. The vehicle model has low dimensionality, and can be efficiently incorporated in a numerical optimization scheme. It is shown that the model is capable of reproducing vehicle responses as those described in Figs 1 and 4.

Rally drivers routinely take advantage of the load transfer from the front to the rear axle and *vice versa* in order to control the yaw motion of the vehicle. As a matter of fact, most of vehicle steering driving at high speed on loose surfaces is done by using load transfer as the primary control input, rather than the direct use of the steering wheel [14]. Because load transfer is so important for vehicle control on loose surfaces, we use a half-car model (Fig. 6) that incorporates longitudinal load transfer effects.

3.1.1. *Equations of Motion*

The equations of motion of the half-car model (Fig. 6) are given as follows.

$$m\ddot{x} = f_{Fx}\cos(\psi+\delta) - f_{Fy}\sin(\psi+\delta) + f_{Rx}\cos\psi - f_{Ry}\sin\psi \tag{1}$$

$$m\ddot{y} = f_{Fx}\sin(\psi+\delta) + f_{Fy}\cos(\psi+\delta) + f_{Rx}\sin\psi + f_{Ry}\cos\psi \tag{2}$$

$$I_z\ddot{\psi} = \left(f_{Fy}\cos\delta + f_{Fx}\sin\delta\right)\ell_F - f_{Ry}\ell_R \tag{3}$$

$$I_F\dot{\omega}_F = T_F - f_{Fx}r \tag{4}$$

$$I_R\dot{\omega}_R = T_R - f_{Rx}r \tag{5}$$

In the above equations m is the vehicle's mass, I_z is the polar moment of inertia of the vehicle, I_i $(i = F, R)$ are the moments of inertia of the front and rear wheels about the axis of rotation, r is the radius of each wheel, x and y are the cartesian coordinates of the center of mass in the inertial frame of reference, ψ is the yaw

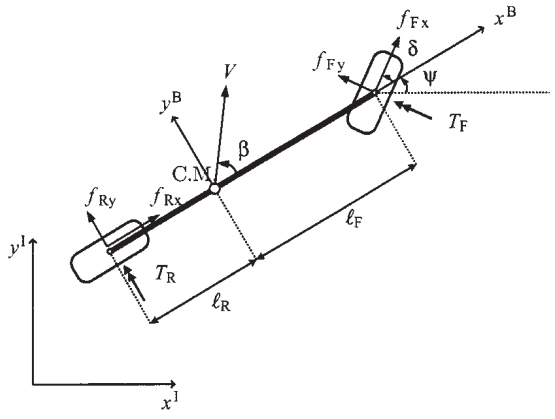

Fig. 6. Half-car vehicle model.

angle of the vehicle, and ω_i $(i = F, R)$ is the angular rate of the front and rear wheel respectively. By f_{ij} $(i = F, R$ and $j = x, y)$ we denote the longitudinal and lateral friction forces at the front and rear wheels, respectively. In this model the inputs are the driving/braking torques T_F and T_R at the front and rear wheels, and δ is the steering angle of the front wheel.

Remark 1: *The equations of motion (1)–(5) are valid only for a vehicle traveling on a flat and level surface. Because actual rally driving usually takes place in roads with various undulations and banks, a more realistic model should use the following equation* in lieu *of (3)*

$$I_z \dot{\omega}_z = (f_{Fy} \cos\delta + f_{Fx} \sin\delta)\ell_F - f_{Ry}\ell_R \tag{6}$$

where

$$\omega_z = \dot{\psi} \cos\phi \cos\theta - \dot{\theta} \sin\phi, \tag{7}$$

and where ϕ and θ are the roll and pitch angles of the vehicle. If the vehicle suspension dynamics are neglected, then ϕ and θ are the same as the bank and grade angles of the driving road. Similarly, in this case equations (1) and (2) need to include the gravity terms owing to nonzero values of ϕ and θ. Therefore, if ϕ and θ are known, it is not hard to incorporate them into a more realistic model used in the optimization discussed later on, but at the expense of increased computational complexity. However, the simplified model in (1)–(5), assuming level road, helps in revealing the primary characteristics of interest without a great loss of generality.

3.1.2. Tire Forces

Assuming linear dependence of the friction forces on the normal load at each wheel, one obtains

$$f_{ij} = f_{iz}\mu_{ij}, \qquad i = F, R,\ j = x, y, \tag{8}$$

where f_{iz} is the normal load at each of the front and rear axles, and μ_{ij} is the longitudinal and lateral friction coefficients of the front and rear tires. The friction coefficients μ_{ij} can be calculated using, for instance, Pacejka's Magic formula [5], normalized by the corresponding axle normal load f_{iz}.

Calculation of the normal load at each axle f_{iz} is straightforward in cases where the suspension dynamics are included in the vehicle model [16, 18]. Otherwise, a static map of the longitudinal acceleration of the vehicle can be used to calculate the normal load transfer from the front to the rear axle and *vice versa* during acceleration and braking [20]. In this work we neglect the suspension dynamics so as not to increase the order of the vehicle model.

Equilibrium of forces in the vertical direction and equilibrium of moments about the point of contact of the rear wheel with the ground result in the following expressions

$$mg = f_{Fz} + f_{Rz} \tag{9}$$

$$mg\ell_R = (f_{Fx}\cos\delta - f_{Fy}\sin\delta + f_{Rx})h + Lf_{Fz}. \tag{10}$$

Equations (9) and (10) can be solved for front and rear axle normal loads:

$$f_{Fz} = \frac{\ell_R mg - hmg\mu_{Rx}}{L + h(\mu_{Fx}\cos\delta - \mu_{Fy}\sin\delta - \mu_{Rx})}, \tag{11}$$

$$f_{Rz} = mg - f_{Fz}, \tag{12}$$

where $L = \ell_F + \ell_R$ and h is the vertical distance of the center of mass of the vehicle from the ground.

3.1.3. Control Inputs

Neglecting engine, transmission, brake and steering system dynamics, we use the following maps to calculate the inputs, T_F, T_R and δ from the nondimensional command signals $u_T \in [-1, 1]$(throttle and brake command) and $u_\delta \in [-1, 1]$ (steering command):

$$\begin{aligned} \delta &= C_\delta u_\delta, \\ T_i &= \begin{cases} -\text{sign}(\omega_i) C_{\text{ibrk}} u_T & \text{for } u_T \geq 0, \\ -C_{\text{iacc}} u_T & \text{for } u_T < 0, \end{cases} \end{aligned} \tag{13}$$

where $i = F, R$. The constants C_δ, C_{Facc}, C_{Racc}, C_{Fbrk} and C_{Rbrk} determine the performance of the steering, engine and brake system. In this work we assume a Front Wheel Drive vehicle, hence $C_{\text{Racc}} = 0$.

The vehicle parameters used in this work are shown in Table 1. The parameters B, C and D refer to Pacejka's Magic Formula tire friction model [5], under the assumption of uniform tire characteristics along the longitudinal and lateral directions.

3.2. Baseline Solution

In this section we calculate the solution to the minimum-time cornering problem for a 90 deg corner on a low μ surface ($\mu = 0.5$), as shown in Fig. 7. The minimum-time cornering problem has been addressed in [18], where numerical optimization was used to compare minimum-time versus maximum exit speed cornering. In [18] independence of the inputs T_F and T_R was assumed.

Table 1. Vehicle Parameters.

Parameter	*Value*
m (kg)	1450
I_z (kg m^2)	2740
ℓ_F (m)	1.1
ℓ_R (m)	1.6
r (m)	0.3
$I_{F,R}$ (kg m^2)	1.8
h (m)	0.4
C_δ (deg)	60
C_{Facc} (Nm)	1000
C_{Racc} (Nm)	0
C_{Fbrk} (Nm)	700
C_{Rbrk} (Nm)	700
B	7
C	1.6
D	0.52

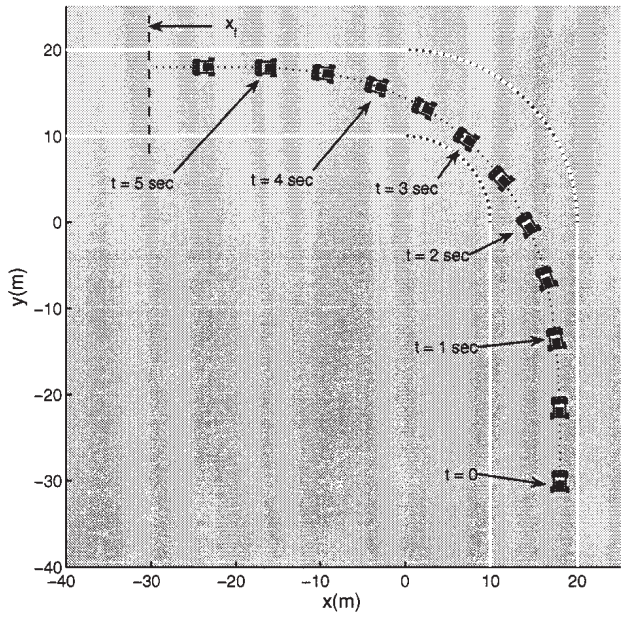

Fig. 7. Baseline minimum-time cornering: vehicle trajectory.

We use collocation to transcribe the optimal control problem to a nonlinear programming problem by discretizing the continuous system dynamics (1)–(5). Consequently, the control inputs are approximated with constant functions during each time interval. The numerical calculations where performed using EZOPT, by Analytical Mechanics Associates Inc., which provides a gateway to NPSOL, a well-known nonlinear optimization program (for details see [11]).

The index to be minimized is the final time

$$J = t_f. \tag{14}$$

By defining

$$C_s(x,y) \triangleq \begin{cases} \sqrt{x^2+y^2} & \text{for } x \geq 0,\ y \geq 0 \\ 15 & \text{otherwise} \end{cases} \tag{15}$$

the road limits of the corner constitute the state inequality constraints of the problem, as follows

$$10 \text{ m} \leq C_s(x,y) \leq 20 \text{ m}. \tag{16}$$

The boundary conditions consist of the fixed initial position, orientation and velocity of the vehicle, partially fixed final position and orientation, and free final speed. The following values were used in the numerical example below

$$\begin{aligned} &x_0 = 18 \text{ m}, \quad y_0 = -30 \text{ m}, \\ &\dot{x}_0 = 60 \text{ km/h}, \quad \dot{y}_0 = 0, \\ &\psi_0 = \pi/2, \quad \dot{\psi}_0 = 0, \quad \psi_f = \pi, \\ &\dot{\psi}_f = 0, \quad x_f = -30 \text{ m}, \quad \dot{y}_f = 0. \end{aligned} \tag{17}$$

The final speed $\dot{x}_f$, as well as the final lateral position y_f are free parameters to be determined by the optimization algorithm.

The minimum-time trajectory, the optimal steering and throttle/brake commands u_δ and u_T, the optimal velocity profile and the vehicle slip angle β are shown in Figs 7, 8(a–d), respectively. The minimum-time trajectory, starts close to the outer edge of the road, approaches the inner edge of the road at the midpoint of the corner, and finally decreases its curvature to meet the specified boundary conditions, taking advantage of the available width of the road. In accordance to the results in [6, 10, 18] the optimal trajectory compromises between the minimum distance (in order to minimize time of travel) and the minimum overall curvature (in order to allow the vehicle to maintain high speeds). There is only partial agreement between the optimal control inputs of Fig. 8(a, b) and the guidelines of Section 2. In particular, hard braking ($0.5 \leq t < 1$ sec), is followed by progressive decrease of the braking input ($1 \leq t < 2$ sec), which is followed by a progressive increase of the throttle command ($2 \leq t < 4.5$ sec), in accordance to the guidelines of Section 2. The optimal steering command consists of an initial transient phase ($0.5 \leq t < 1.5$ sec), an approximately constant value ($1.5 \leq t < 4.5$ sec), and a final transient counter-steer ($4.5 \leq t < 5.5$ sec) at the end of the cornering maneuver. Furthermore, the steering profile does not capture the characteristic progressive increase and decrease of the steering command as described at Section 2, and also seen in Fig. 5(a). Finally, the vehicle slip angle β remains small throughout the minimum-time trajectory, as opposed to the high vehicle slip angle evident in Fig. 5(e).

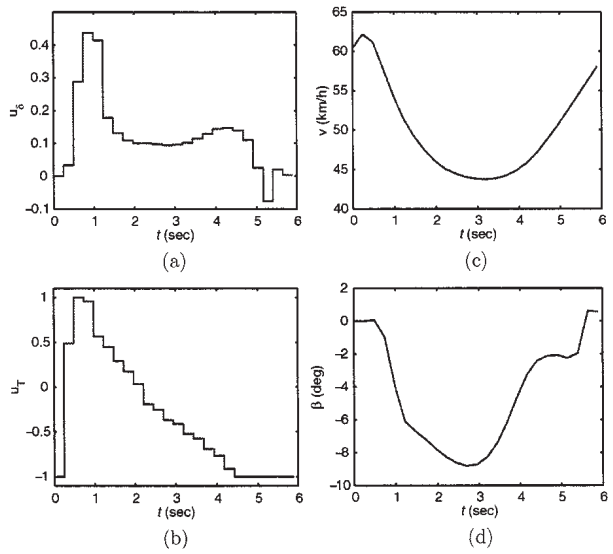

Fig. 8. Baseline minimum-time cornering. (a) normalized steering command; (b) normalized braking command; (c) vehicle speed; (d) vehicle slip angle.

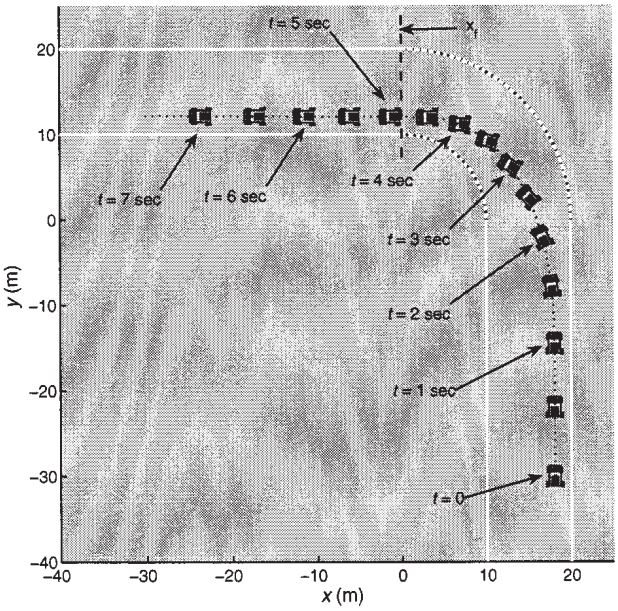

Fig. 9. Trail-braking cornering: vehicle trajectory.

3.3. Trail-Braking

In this section we consider an alternative optimization scenario to the one presented in Section 3.2. The scenario is motivated by the challenges encountered during high-speed rally driving. Unlike closed circuit driving of high-performance vehicles (e.g., F1), off-road rally-racing involves an unpredictably changing environment and lack of detailed information about the condition of the road. Rally drivers bring their vehicles in a controllable straight line driving state early on into the corner, a strategy that allows them to react to emergencies and unexpected changes in the environment after each corner.

Consider again the 90 deg corner of Section 3.2. We will solve the minimum-time problem using the same cost (14), state constraints (16) and boundary conditions (17) as before, except for x_f, which is now set to $x_f = 0$. Namely, we enforce the condition that the vehicle reaches straight line driving condition ($\dot{y}_f = 0$, $\psi_f = \pi$ and $\dot{\psi}_f = 0$) at 30 m *ahead* of the previous final state. Once again, the final speed $\dot{x}_f$, as well as the final lateral position y_f are free parameters.

The minimum-time trajectory, the optimal steering and throttle/brake inputs, the optimal velocity profile and the vehicle slip angle are shown in Figs. 9, 10(a–e) respectively (dashed curves). We observe that the vehicle exits the corner close to the inner limit of the road (Fig. 9), rather than taking advantage of the whole width of the road as in Fig. 7. We also observe that the apex is now at the end of the path ($x = 0$ m) rather than at the midpoint of the corner. The optimal control inputs shown in Fig. 10(a) and 10(b) are

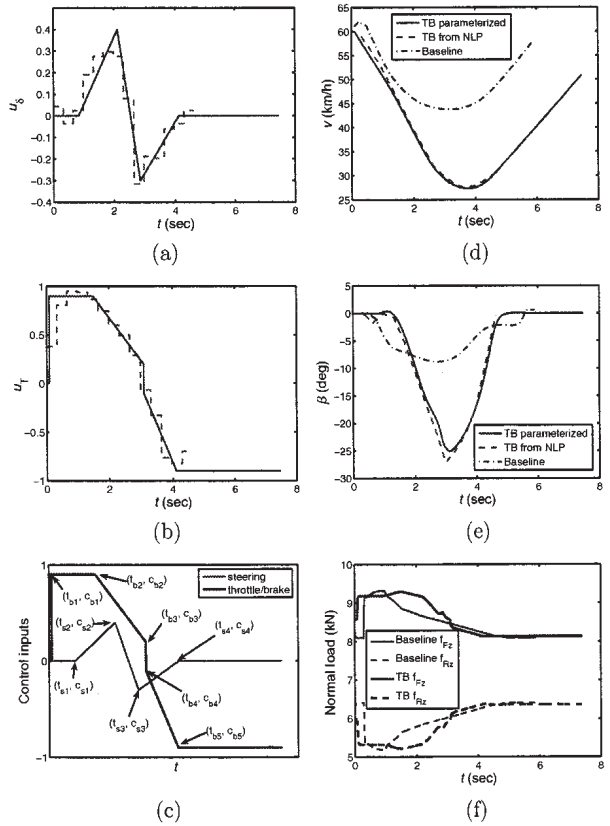

Fig. 10. Trail-braking cornering. (a) normalized steering command; (b) normalized braking command; (c) input parameterization; (d) vehicle speed; (e) vehicle slip angle; (f) front and rear axle normal loads.

in qualitative agreement with the description of Section 2 and Fig. 5(a–c). In particular, hard braking ($0.1 \leq t < 1.5$ sec), is followed by a progressive decrease of the braking input ($1.5 \leq t < 3$ sec). The steering command increases toward the direction of the corner ($1 \leq t < 2$ sec), then decreases with subsequent counter-steering ($2 \leq t < 3$ sec). A progressively increasing throttle command is applied and counter-steering is reduced to zero ($3 \leq t < 4$ sec). As shown in Fig. 10(e), the vehicle negotiates the corner with a high slip angle. The optimal solution in this case follows closely a TB trajectory.

Next, we demonstrate that the previous TB maneuver can be generated using a simplified numerical optimization formulation. In particular, we approximate the control inputs u_δ and u_T using fixed sequences of constant and ramp functions, determined by two sets of parameters (t_{si}, c_{si}) and (t_{bj}, c_{bj}), as in Fig. 10(c). We re-solve the minimum-time problem using (t_{si}, c_{si}) and (t_{bj}, c_{bj}) as the parameters to be optimized (instead of the control inputs at each time step). This simplified optimization scheme will be described in greater detail in the following section. The parameterized steering and throttle/brake control inputs, the velocity profile and the vehicle slip angle are shown in Fig. 10(a, b, d, e) respectively (solid lines). We observe that using the simple parameterization of the control inputs of Fig. 10(c) we are able to reproduce essentially the same solution as the one using nonlinear programming. For comparison, we have included in Fig. 10(d, e) the velocity profile and vehicle slip angle of the Baseline solution obtained in the previous section.

Comparing the Baseline solution of the previous section with the TB, we observe that the Baseline solution reaches the $x = -30$ m position in approximately 5.8 sec, where as the TB solution reaches the same point in 7.5 sec. Nonetheless, the TB maneuver is the minimum-time solution when we require that the vehicle completes the cornering maneuver and returns to a straight line driving condition much earlier when compared to the Baseline solution. Furthermore, TB involves significantly larger vehicle slip angles than the Baseline solution, as seen in Fig. 10e). Although in the Baseline solution the vehicle utilizes the whole width of the road (Fig. 7), TB results in a "late-apex" trajectory (Fig. 9). Finally, in Fig. 10(f) we see that the changes in the normal load balance between front and rear axles are of higher rate of change (more aggressive) in the case of TB than the Baseline solution. The load transfer from the rear to the front axle during braking results in more oversteer and a more aggressive change in the vehicle slip angle during cornering. Conversely, the load transfer from the front to the rear axle during acceleration results in more understeer and is used to stabilize the vehicle while exiting the corner.

4. Input Parameterization and High-fidelity Validation

In the previous sections we used a simple model to numerically solve the minimum-time cornering problem for a variety of terminal boundary conditions. The results obtained by this optimization algorithm corroborate the TB characteristics observed using actual test data. Nonetheless, owing to the simplicity of the model and the fixed geometry used, there is still a need to validate these numerical results against more sophisticated models that capture all effects that were neglected during optimization, and to do so for a variety of corner geometries. In this section we reproduce TB maneuvers *via* numerical optimization using a high fidelity vehicle model for a variety of corner geometries. As the main simulation engine we use CarSim [4], a program that allows us to integrate the full-car vehicle dynamics of an All-Wheel-Drive sedan into the overall optimization scheme. The vehicle model incorporates realistic engine, transmission and braking system characteristics. Besides the steering command, the control inputs to be optimized are independent throttle and brake commands (rather than the composite control input u_T used in the previous sections). A direct transcription of the system equations used in CarSim is out of the question. Furthermore, working directly with the original input functions (which normally have to be discretized over time into small time intervals) also leads to a problem of high computational complexity. For this reason, in this section we use an alternative method to solve the optimization problem. Specifically, instead of NPSOL we use a Newton method, where a cumulative error is iteratively optimized by numerically computing its gradients with respect to a given set of free (control) optimization parameters. Furthermore, in order to reduce the optimization search space, we introduce a simple parameterization of the control commands in accordance to the description of Section 2.

4.1. Input Parameterization

We propose a steering, braking and throttle command parameterization for the TB maneuver as shown in Fig. 11. According to the discussion in Section 2, the TB maneuver starts with the vehicle braking hard while driving straight (see braking command in Fig. 11 for

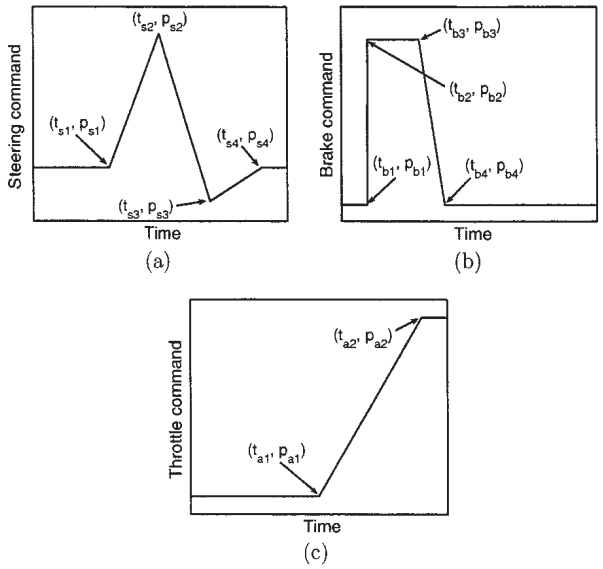

Fig. 11. Parameterized (a) steering, (b) braking and (c) throttle inputs for Trail-Braking.

$t_{b2} \leq t < t_{b3}$). The driver then increases steering toward the direction of the corner ($t_{s1} \leq t < t_{s2}$) and progressively decreases braking ($t_{b3} \leq t < t_{b4}$). Next, the driver decreases steering and counter-steers ($t_{s2} \leq t < t_{s3}$), while progressively applying the throttle ($t_{a1} \leq t \leq t_{a2}$) to stabilize the vehicle at the exit of the corner. The steering angle is reduced to zero ($t_{s3} \leq t \leq t_{s4}$) and the vehicle exits the corner while accelerating hard ($t > t_{a2}$). The driver commands of Fig. 11 are steering angle, throttle position and brake pressure normalized by the corresponding maximum allowable value.

4.2. Optimal Control Formulation

A simplified numerical optimization scheme was used to reproduce TB maneuvers along several corner geometries using the control input parameterization shown in Fig. 11. The dynamics of the vehicle correspond to a light weight (1000 kg), All-Wheel-Drive (50/50 torque distribution), 2.5 L-115 kw engine sedan, whereas the friction coefficient of the road was assumed to be $\mu = 0.5$. for all corner geometries we assumed an inner corner radius of 10 m and an outer corner radius of 20 m. The corner angles are 60, 90, 135, and 180 deg. The initial conditions for all optimization scenarios were the same.

The vehicle starts at 45 m from the center of the corner, traveling straight with a speed of 70 km/h. The lateral velocity, slip angle and yaw rate are all initially zero. The vehicle starts at a lateral distance of 2 m from the outer limit of the road. The optimization takes place until the vehicle reaches 15 m beyond the center of the corner. It is desired that the vehicle will reach this

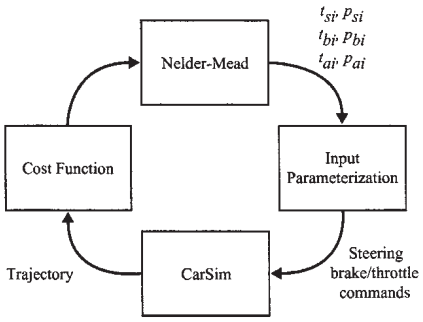

Fig. 12. The numerical optimization scheme using the proposed input parameterization and vehicle response calculations with CarSim.

final position traveling straight with zero lateral velocity, slip and yaw rate. It is also desired that the vehicle remains close to the inner limit of the road such that a "late apex trajectory" is enforced, in accordance to the empirical guidelines. The final velocity of the vehicle is a free parameter in our optimization.

As in Section 3.2, we reproduce the TB maneuver as a special case of the minimum-time cornering problem, subject to the above boundary conditions. We assume that the trajectory is known at discrete times $0 = t_0 < t_1 < \cdots < t_N = t_f$ and we wish to find the optimal parameters t_{si}, p_{si}, t_{bi}, p_{bi}, t_{ai}, p_{ai}, that minimize the following cost function:

$$\hat{J} = W_t t_f + W_r e_r + W_d e_d(t_f) + W_\psi e_\psi(t_f) + W_v e_v(t_f) + W_y e_y(t_f), \tag{18}$$

where, t_f is the final time, $e_r = \sum_{k=1}^{N} e_r(t_k)$ is the cumulative absolute value of the position error from the road limits, $e_d(t_f)$ is the absolute value of the lateral deviation of the vehicle from the inner limit of the road at t_f, $e_\psi(t_f)$ is the final absolute orientation error, $e_v(t_f)$ is the final absolute lateral velocity of the vehicle, and $e_y(t_f)$ is the final absolute yaw rate error of the vehicle. The weights W_i $(i = t, c, d, \psi, v, y)$ are used for nondimensionalization and to adjust the relative significance between the terms in the right-hand-side of (18). The optimization was performed in Matlab using an unconstrained nonlinear minimization algorithm (Nelder-Mead) as shown in Fig. 12.

In Fig. 13 the optimal steering, braking and throttle commands are shown. Notice that certain parameters (p_{si}, p_{bi} and p_{ai}) are common to all cases. We have deliberately fixed the values of these parameters in order to reduce the optimization search space further. This simplified optimization scheme, nonetheless, was successful at reproducing TB maneuvers for all corner geometries. In Fig. 14 we show the velocity profile and vehicle slip angle along each optimal trajectory. In the same figure we also show the front and rear normal

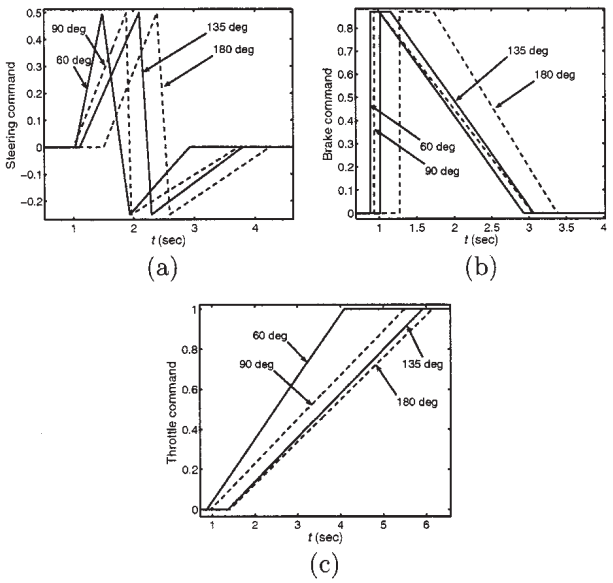

Fig. 13. Optimal steering, brake and throttle inputs through the 60, 90, 135 and 180 deg corners.

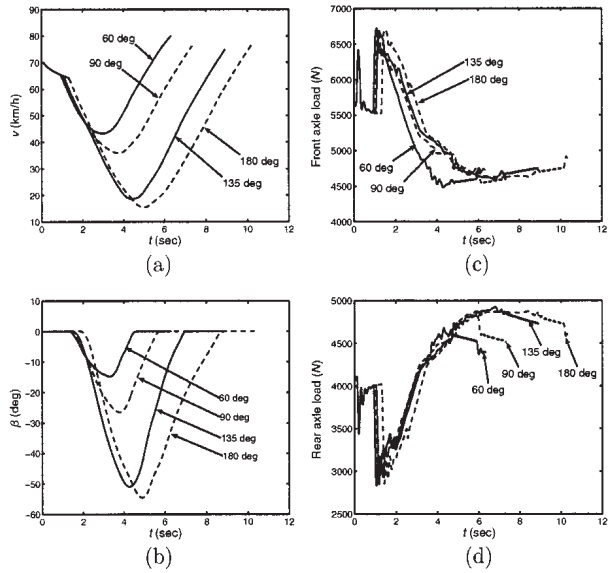

Fig. 14. Optimal vehicle speed (a), vehicle slip angle (b), front and rear axle normal loads (c), (d) through the 60, 90, 135 and 180 deg corners.

loads in order to demonstrate the longitudinal load transfer that takes place during acceleration and deceleration, and which plays a key role in a TB maneuver, as described earlier. As expected, a braking command results in load transfer from the rear to the front axle, assisting in the initial rotation of the vehicle. Conversely, a throttle command results in load transfer from the front to the rear axle, and controls the yaw motion while exiting the corner.

Fig. 15 shows the optimal trajectories of the vehicle along the 60, 90, 135 and 180 deg corners respectively. The simulation continues up to 45 m distance after the center of the corner (that is, 30 m after the end of the optimization) with maximum acceleration, in order to demonstrate that the boundary conditions at the end of the corner have been satisfied. Fig. 16 also demonstrates the resulting optimal trajectories using the 3D rendering tool of CarSim.

These numerical results demonstrate the validity of the empirical guidelines introduced in Section 2.1 and the proposed input parameterization for a variety of corner geometries.

5. Conclusions

In this paper we have initiated a mathematical analysis of rally racing techniques. We have concentrated on a high speed cornering technique used extensively by rally drivers, namely TB. We explored the optimality properties of TB by formulating several minimum-time cornering scenarios, which were solved using nonlinear programming. We concluded that TB corresponds to the minimum-time cornering solution when the vehicle is required to return to the straight line driving condition right after it reaches the geometric end of the corner. The solution generated by the optimization scheme showed excellent agreement with the guidelines provided by expert rally drivers, as well as with experimental data. Finally, and in order to reduce the numerical complexity during optimization, we proposed a parameterization of the control inputs that can be used to reproduce TB maneuvers for a variety of corner geometries.

Acknowledgments

The authors would like to thank Mr. Tim O'Neil and his colleagues at the Team O'Neil Rally School and Car Control Center for the instructional courses and informative discussions on rally driving, as well as for generously offering use of their facilities and vehicles, and finally participating in the data collection process. The authors would also like to thank Mr. Christopher Nave and Mr. Steve Hermann from the Research and Advanced Engineering Department of Ford Motor Company for their valuable assistance during the experiments. This work has been supported by Ford Motor Company through the URP program and the ARO through award no. W911NF-05-1-0331.

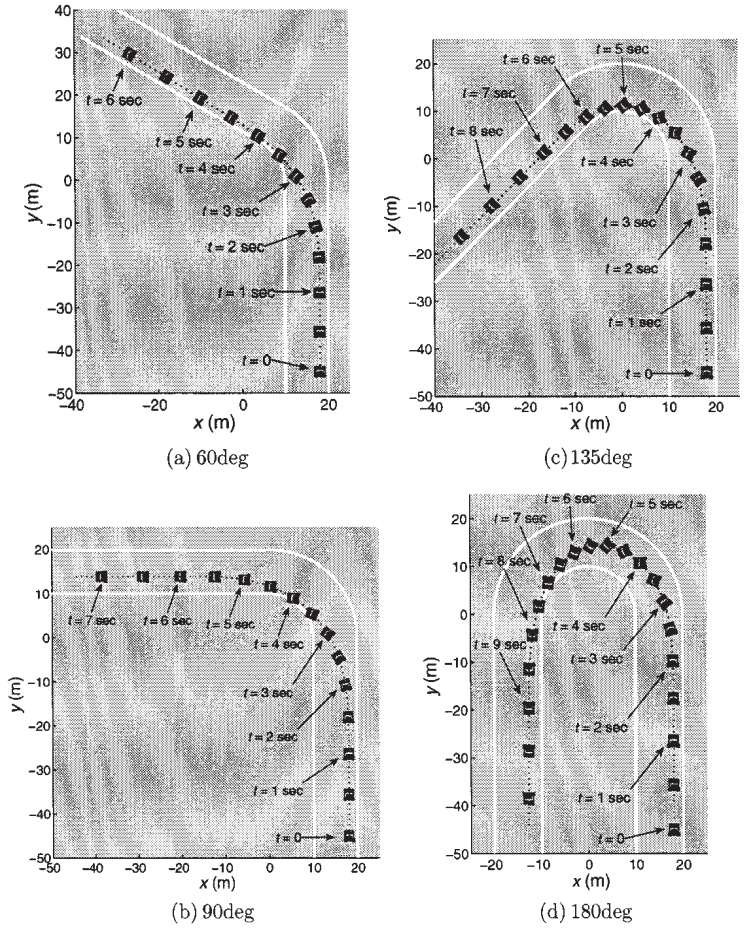

(a) 60deg (c) 135deg

(b) 90deg (d) 180deg

Fig. 15. Optimal trajectory through 60, 90, 135 and 180 deg corners.

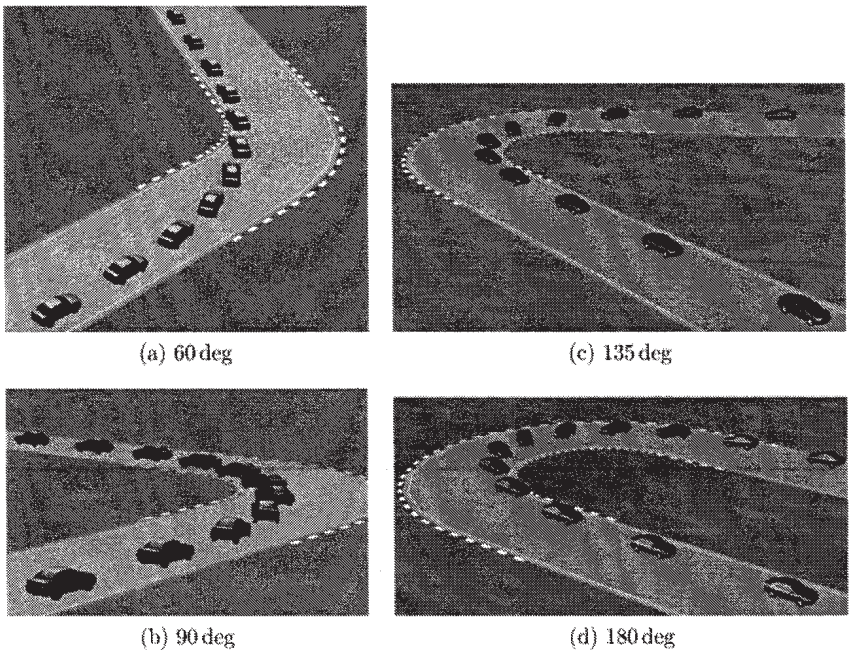

(a) 60 deg (c) 135 deg

(b) 90 deg (d) 180 deg

Fig. 16. TB through the 60, 90, 135, and 180 deg corners.

References

1. www.darpa.mil/grandchallenge05/index.html
2. www.oxts.com/
3. www.race-technology.com/
4. Mechanical Simulation Corporation, Ann Arbor, MI
5. Bakker E, Nyborg L, Pacejka HB. Tyre modelling for use in vehicle dynamics studies, 1987. SAE Paper No. 870421
6. Casanova D, Sharp RS, Symonds P. Minimum time manoeuvring: The significance of yaw inertia. *Veh Syst Dyn* 2000; 34: 77–115
7. Casanova D, Sharp RS, Symonds P. On minimum time optimisation of formula one cars: The influence of vehicle mass. In Proceedings of AVEC 2000, Ann-Arbor, MI, August 22–24, 2000
8. Frazzoli E, Dahleh MA, Feron E. Real-time motion planning for agile autonomous vehicles. *J Guid, Control Dyn* 2002; 25(1): 116–129
9. Frazzoli E, Dahleh MA, Feron E. Maneuver-based motion planning for nonlinear systems with symmetries. *IEEE Trans Robot* 2005; 21(6): 1077–1091
10. Gadola M, Vetturi D, Cambiaghi D, Manzo L. A tool for lap time simulation. In Proceedings of SAE Motorsport Engineering Conference and Exposition, Dearborn, MI, 1996
11. Gill PE, Murray W, Saunders MA, Wright MH. *User's Guide for NPSOL (version 4.0)*. Department of Operations Research, Stanford University, CA, 1986. Report SOL 86–2
12. Hendrikx JPM, Meijlink TJJ, Kriens RFC. Application of optimal control theory to inverse simulation of car handling. *Veh Syst Dyn* 1996; 26: 449–461
13. Lepetic M, Klancar G, Skrjanc I, Matko D, Potocnic B. Time optimal path planning considering acceleration limits. *Robot Auton Syst* 2003; 45: 199–210
14. O'Neil T, 2006. private communication
15. O'Neil T. *Rally Driving Manual*. Team O'Neil Rally School and Car Control Center, 2006
16. Velenis E. *Analysis and Control of High-Speed Wheeled Vehicles*. PhD thesis, School of Aerospace Engineering, Georgia Institute of Technology, 2006
17. Velenis E, Tsiotras P. Optimal velocity profile generation for given acceleration limits: Theoretical analysis and receding horizon implementation. *J. Optim Theory and Appl* 2008; 138: 275–296
18. Velenis E, Tsiotras P. Minimum time vs maximum exit velocity path optimization during cornering. In 2005 IEEE International Symposium on Industrial Electronics, Dubrovnic, Croatia, June 2005, pp. 355–360
19. Velenis E, Tsiotras P. Optimal velocity profile generation for given acceleration limits: The half-car model case. In 2005 IEEE International Symposium on Industrial Electronics, Dubrovnic, Croatia, June 2005
20. Villela MG. *Nonlinear Modeling and Control of Automobiles with Dynamic Wheel-Road Friction and Wheel Torque Inputs*. M.S. thesis, School of Electrical and Computer Engineering, Georgia Institute of Technology, 2004